

Wheat domestication gene *Q* interplays with *TaARF12* to antagonistically modulate plant architecture by integrating multiple hormone homeostasis

Bingyan Liu¹, Mengjing Sun¹, Ke Wang¹ , Yingjie Bian¹, Yuqing Che¹, Jindong Liu¹, Xumei Luo¹, Siyang Liu¹, Lina Xie¹, Lingli Li¹, Kejia Qu¹, Yuheng Chao¹, Rui Che¹, Xingguo Ye¹ , Xianchun Xia¹ , Long Mao¹ , Zhonghu He^{1,2} , Aili Li¹  and Shuanghe Cao¹ 

¹State Key Laboratory of Crop Gene Resources and Breeding/National Wheat Improvement Center/National Key Facility for Crop Gene Resources and Genetic Improvement, Institute of Crop Sciences, Chinese Academy of Agricultural Sciences, Beijing, 100081, China; ²International Maize and Wheat Improvement Center (CIMMYT) China Office, Chinese Academy of Agricultural Sciences, Beijing, 100081, China

Authors for correspondence:
Shuanghe Cao
Email: caoshuanghe@caas.cn

Aili Li
Email: liaili@caas.cn

Zhonghu He
Email: hezonghu02@caas.cn

Received: 6 July 2025
Accepted: 24 July 2025

New Phytologist (2025)
doi: 10.1111/nph.70487

Key words: domestication gene *Q*, functional dissection, plant architecture, wheat, yield potential.

Summary

- Wheat domestication gene *Q* controls threshability and also pleiotropically affects plant morphogenesis. However, its specific roles in modulating plant architecture and the underlying mechanisms remain unclear.
- We dissected *Q* effects on plant architecture using transgenic overexpression and knockout assays. The analyses of micromorphological and dynamic imaging, physiological productivity, multi-omics, and molecular interaction were performed to dissect the underlying regulatory mechanism. Allelic variation and genetic effect assays were employed to identify desirable haplotypes.
- The domesticated *Q* allele *5AQ* in wild-type lines optimized plant architecture and endowed yield gain by modulating cell size of stem internodes and flag leaves, tiller initiation and outgrowth, and photosynthetic capacity. *Q* regulated many homologs of previously reported functional genes controlling plant architecture, multiple hormone homeostasis, and cell wall components. *Q* upregulated plant architecture regulators *TaARF12-2B* and *TaARF12-2D* by binding to the promoters. However, *Q* and the *TaARF12* genes antagonistically modulate plant architecture. The favorable haplotypes of *TaARF12-2B* and the functional variation site were identified, and their origin, spread, and distribution were also traced.
- These findings specify the *Q* function in controlling plant architecture and yield formation, broaden insights into the underlying mechanism, and provide new molecular tools for wheat improvement.

Introduction

Wheat (*Triticum aestivum*), one of the most important staple crops, is generated from two polyploidization events involving the genera *Triticum* and *Aegilops* (IWGSC, 2014). In wild wheat progenitors, the spike is nonfree threshing, that is, the grains are covered by tough glumes that remain attached to the seeds after threshing. Domestication gave rise to free-threshing spikes with soft glumes. Wheat *Q* genes on chromosomes 5A controlling threshability encode AP2 (APETALA2) transcription factors, homologous to IDS1 (indeterminate spike 1) in maize and rice. The domesticated *Q* allele *5AQ* originated from two mutations in *5Aq*, A-to-G at position 985 in the 8th exon and C-to-T at position 1254 in the 10th exon. The former is a missense mutation (valine to isoleucine), which possibly increased homodimer formation (Simons *et al.*, 2006), and the latter causes no amino acid change but attenuates miRNA172-mediated cleavage of the

transcript (Liu *et al.*, 2018). *5Bq* and *5Dq* on chromosomes 5B and 5D, respectively, are orthologs of *5AQ*. In polyploid wheat, *5AQ* plays a major role in conferring domestication-related traits, whereas *5Bq* is a pseudogene and *5Dq* has been subfunctionalized (Zhang *et al.*, 2011).

Plant architecture is of agronomic importance, greatly influencing crop cultivation suitability and yield potential (Yang & Hwa, 2008). *Q* genes not only alter threshability (Faris *et al.*, 2003) but also affect plant architecture traits, such as plant height (Simons *et al.*, 2006; Debernardi *et al.*, 2020), spike length (Simons *et al.*, 2006), and tiller number (Förster *et al.*, 2013). Thus, *Q* is thought to be the most important domestication gene in cultivated wheat. Previous studies focused on dissecting the mechanism of *Q* modulating spike development and morphogenesis, such as floral initiation (Debernardi *et al.*, 2022), soft glume (Song *et al.*, 2019), and spikelet compactness (Liu *et al.*, 2018). However, the specific function of *Q* in

modulating plant architecture and grain formation as well as the underlying mechanism is largely unknown. In this study, we comprehensively specified the function of *Q* in modulating plant morphogenesis and concomitant yield gain using transgenic assays. The developmental causes for resulting phenotypic changes were explored by micromorphological and dynamic imaging. The underlying regulatory mechanisms were further dissected by physiological, biochemical, and transcriptome analyses. A large number of genes in all tested tissues, including stem internodes, tillers, and leaves, were regulated by *Q*, suggesting that it is a master switch controlling plant architecture. Among them, many genes were involved in multiple hormone homeostasis and metabolism of lignin and cellulose, two major structural components of the cell wall. Notably, *Q* regulated auxin response factor (ARF) genes *TaARF12* on homoeologous group 2 via direct binding to the promoters, forming a regulatory module controlling plant architecture. The favorable alleles of *TaARF12* on chromosomes 2B were identified by analyses of genetic effect. We further clarified the sites causing functional variation in the favorable alleles and developed a diagnostic molecular tool for marker-assisted selection in wheat breeding.

Materials and Methods

Plant materials, field trials, and phenotypic evaluation

Previously created *5AQ* knockout (*Q*-KO) lines in wheat cultivar (cv.) Fielder and *5AQ* overexpression (*Q*-OE) lines using the cv. CB037 were available from our earlier studies (Song *et al.*, 2019; H. Liu *et al.*, 2020). These materials were grown in transgene test sites at Beijing (40°2'N, 116°2'W) and Shijiazhuang (38°03'N, 114°) during the 2022–2023 cropping season. Each line was planted in 5 × 2-m row plots at 21 plants per row. Field management followed local practices. Plant architecture traits of transgenic lines and their respective controls, including plant height (excluding awns), stem thickness, tiller angle, tiller number, spike number per plant, flag leaf size and angle, awn length, and spike length (excluding awns) were investigated following Xu *et al.*, 2023. Ineffective tiller per plant is total tiller minus spike number per plant (productive tiller), and ear-bearing tiller rate is the ratio of spike number to total tiller. The degree of plant uniformity was quantified according to the following formula: S/X , where X represents the mean of all tiller height of individual plants and S denotes the SD. Grain yield and yield component traits were also scored according to Li *et al.* (2019).

A diverse panel of 166 wheat cultivars from the Huang-Huai valley region was used to validate the genetic effects of major haplotypes of target genes. Agronomic traits of panel members were available from Li *et al.* (2019). Forty-two tetraploid wheat accessions were used to trace the origin of favorable haplotypes, including 11 *T. durum*, 22 *T. dicoccoides*, and 9 *T. dicoccum* accessions (http://wheat.cau.edu.cn/Wheat_SnpHub_Portal/). A total of 978 wheat cultivars and landraces from world-wide sources were used to investigate the distribution of favorable haplotypes (Bian *et al.*, 2023).

Histochemical staining and microscopic imaging

Uppermost internodes and flag leaves were harvested at 15 d post-anthesis and fixed in FAA solution (70% alcohol, 5% acetic acid, and 0.02% formaldehyde) for at least 24 h. The samples were dehydrated, embedded in melted paraffin, and cut into 4-μm slices, which were stained with solid green dye for investigating anatomical structures in transverse and longitudinal stem sections, and longitudinal flag leaf sections in Servicebio (<https://www.servicebio.com/>). The cells of stem internodes and flag leaves were imaged with a digital Panoramic™ MIDI scanner (3DHitech Ltd, Budapest, Hungary). Lower epidermis sections of flag leaves were prepared by initial scraping of leaves immersed in FAA solution, dissociation with 20% sodium hypochlorite for 3 min, secondary scraping and transferring onto slides, and then imaged by a Leica DM4B upright microscope. Microstructural phenotypes, including cell length, width, thickness, and number, were scored by IMAGEJ (<https://imagej.nih.gov/ij/index.html>). Three biological replicates per sample were used in each experiment.

Measurement of photosynthetic rate, Chl content, and stem strength

A portable infrared gas analyzer system (LI-6400XT; Li-Cor, Lincoln, NE, USA) was used to measure the net photosynthetic rate (Pn) of flag leaves at the grain fill stage. Upon measuring Pn, photosynthetic light flux density (PPFD), ambient temperature, and CO₂ concentration were set to 1000 mol m⁻² s⁻¹, 25–28°C, and 400 ppm, respectively. Chlorophyll content was measured by a SPAD-502 Chl meter (Minolta, Tokyo). Stem strength was determined by a TP-YYD-1 dynamometer (https://www.tpy.net/products/show_96.html), used to exert a gradual force in a vertical direction on the stem. The maximum reading value attained when stems were broken was deemed to be the stem strength score.

Quantitative analysis of hormone, cellulose, and lignin

Endogenous hormones, including auxin, cytokinin (CTK), abscisic acid (ABA), and gibberellin (GA), were extracted from tiller buds at Zadoks growth stage (ZGS) 26, leaves at ZGS 37, and stems at ZGS 49 of *Q*-KO lines and Fielder by acetonitrile solution extraction. In total, 50 mg of the material was extracted with 1 ml cold 50% acetonitrile (Merck, Darmstadt, German). The extract was then purified by the QuEChERS method (Perestrelo *et al.*, 2019; <https://www.quechers.eu/>). The sample was loaded onto the cartridge and concentrated by the Water Bath Nitrogen Blower (http://www.naaiyiqi.com/products_9/59.html) and stored at –20°C until used. The resultant hormones were dissolved in methanol for quantitative analysis. Standard addition and stable isotope dilution methods were used in quantifying plant hormones. Deuterated analogs of the plant hormones (Sigma) were diluted in methanol solutions at final concentrations of 0.1, 0.2, 0.5, 2, 5, 20, 50, and 200 ng ml⁻¹ for preparing standard curves. Purified extracts were separated on the Poroshell 120 Reversed-Phase UHPLC Column

(2.1×150 , $2.7 \mu\text{m}$; Agilent) with a linear methanol gradient for 10 min at a flow rate of 0.3 ml min^{-1} and a column oven of 40°C in the Perkin Elmer QSight LX50 UHPLC. Perkin Elmer QSight 420 Triple Quad MS was used to determine hormones through scanning the analyte in multiple reaction detection (MRM) modes according to the user manual of the manufacturer (https://perkinelmer.cl/wp-content/uploads/2018/05/BRO_QSight-Triple-Quad-LCMSMS_012855_02.pdf). Hormones sequentially enter the ion source, and then, each component is ionized by means of electric spray ionization (ESI) and is accelerated to enter the QSight 420, including three tandem mass spectrometers: Q1, Q2, and Q3. Q1 is set on the specific parent m/z to separate ionized hormones according to the mass-to-charge ratio (m/z); Q2 is the collision chamber, where the collision energy is set to produce the optimal diagnostic charged fragment of that parent ion, and Q3 has two functions: a quadrupole and a linear ion trap, which can separate molecular ions or fragment ions based on their mass-to-charge ratios. The extraction, purification, concentration, and quantification of hormones were conducted in Nanjing Webiolotech Testing Technology Co., Ltd (<https://www.webiolotech.com/en/>). Finally, the analyte was quantified using a standard curve. The bioactive GA isoforms, GA1, GA3, GA4, and GA7 were measured. For CTK species, *trans*-zeatin riboside, dihydrozeatin riboside, N6-(delta2-isopentenyl) adenosine (IPA), Zeatin, *trans*-zeatin (Tzeatin), and isopentenyl adenine (IP) were quantified. All tested components of GA or CTK were merged to statistically analyze the change between contrasting lines. We also quantified indole-3-acetic acid (IAA) and ABA.

The quantification of cellulose and lignin was carried out using the anthrone sulfate colorimetric method (<https://biochemden.com/anthrone-method/>) and concentrated sulfuric acid method (Kline *et al.*, 2010), respectively.

RNA-seq assays

Tiller buds, flag leaves, and stem internodes of *Q*-KO lines and Fielder were collected at ZGS 26, 37, and 49, respectively. Extraction of total RNA from two biological replicates, library construction, and second-generation sequencing were conducted by Novogene (<https://www.novogene.com>). mRNA was purified from total RNA using poly-T oligo-attached magnetic beads (S1419S; NEB, Frankfurt am Main, Hessen Land, German) and sequenced on an Illumina HiSeq 4000 sequencing platform at 10-Gb sequencing depth. Reference genome and gene model annotation files were downloaded from the Chinese Spring genome website (ftp://ftp.ensemblgenomes.org/pub/release-44/plants/gtf/triticum_aestivum). The expected number of fragments per kilobase of transcript sequence per million mapped reads was used to estimate gene expression levels. The software DESeq2 was used to calculate adjusted *P* values with a negative binomial distribution model for determining significant difference in gene expression levels (Love *et al.*, 2014). The criteria for determining differentially expressed genes (DEGs) were $P < 0.05$ and $|\log_2(\text{FoldChange})| \geq 1$. Heatmaps were produced to display expression patterns of DEGs by the TBTOOLS (Chen *et al.*, 2020).

RNA extraction and quantitative PCR (qPCR) experiments

Leaves from wheat cultivars at the seedling stage were sampled to extract RNA by an EasyPure Plant RNA Kit (ER301; Transgene, Beijing, China). Total RNA ($1 \mu\text{g}$) was used as a template to synthesize first-strand cDNA using a PrimeScript RT Reagent kit (Takara, Shiga, Japan). qPCR was performed in $20 \mu\text{l}$ reaction volumes consisting of $2 \mu\text{l}$ cDNA template, $0.4 \mu\text{l}$ of each primer ($10 \mu\text{M}$), $7.2 \mu\text{l}$ ddH₂O and $10 \mu\text{l}$ $2\times$ Universal SYBR Green Fast qPCR Mix (RK21203; ABclonal, Wuhan, China) on a Bio-Rad CFX system. The wheat actin gene (*TraesCS1B02G283900*) was used as an internal control. Relative expression of target genes was calculated using the $2^{-\Delta\Delta\text{CT}}$ method (Livak & Schmittgen, 2001). Each wheat cultivar was analyzed with three biological replicates. All primers used in this study are listed in Supporting Information Table S1.

Y1H and dual-luciferase reporter assays

Yeast one-hybrid (Y1H) analysis was performed as described in Lin *et al.* (2007). We inserted the coding sequence (CDS) of 5AQ from Fielder into the pB42AD vector (cat. no.: ZT0295; Clontech, Mountain View, CA, USA) between the *Eco*RI and *Xho*I restriction sites to produce pB42AD-Q as 'prey'. Each *TaARF12* promoter (*c.* 500-bp upstream of the start codon) was separated into three fragments, and each fragment was cloned into the pLacZi reporter vector (cat. no.: 631707; Clontech) to generate the 'bait' through double digestion with *Eco*RI and *Kpn*I. Each 'bait' and 'prey' pair was co-transformed into yeast strain EGY48. Transformants were cultured on SD-Trp/-Ura plates at 30°C for 3 d and then transferred into X-Gal (5-bromo-4-chloro-3-indolyl β -D-galactopyranoside) plates for galactosidase activity analysis. The pB42AD and pLacZi empty vectors combined with 'bait' and 'prey', respectively, were co-transformed into EGY48 as negative controls.

The promoter (1.0-kb upstream of the start codon) of each *TaARF12* gene was inserted into the pGreenII 0800-LUC between the *Nco*I and *Kpn*I restriction sites. The pGreenII 0800-LUC vector included two reporters, firefly luciferase (LUC) and renilla luciferase (REN), driven by the *TaARF12* and *CaMV35S* promoters, respectively. The REN reporter was used as an internal control to normalize LUC activity. The full-length CDS of 5AQ was inserted into pGreenII 62-SK to generate an effector by double digestion with *Eco*RI and *Xho*I. The resultant constructs were transformed into *Agrobacterium tumefaciens* strain GV3101 and co-infiltrated into tobacco leaves as described in Xie *et al.* (2023). LUC signals were imaged using the Tanon-5200Multi apparatus (Tanon, Shanghai, China). LUC activity was quantified with a Dual-Luciferase Assay Kit (Promega) according to the manufacturer's recommendations. Relative LUC activity was calculated by the ratio of LUC/REN. Each sample was tested in three replications.

Identification of allelic variations and KASP marker development

Sites of variation in the target genes were retrieved from the WheatUnion database, in which MP and NC-CC panels were

selected as samples, and the ranges of upstream or downstream open reading frames (ORFs) of target genes were 2000 bp (<http://wheat.cau.edu.cn/WheatUnion/>). Their major haplotypes were also defined in WheatUnion. The flanking sequences of the target variation sites were submitted to POLYMARKER (<https://www.polymarker.info/>) to design KASP primers. KASP genotyping was conducted following Bian *et al.* (2023).

Promoter activity assays in *Nicotiana benthamiana*

TaARF12 promoters (1.0-kb upstream of the start codon) with target variations were cloned into the pGreenII 0800-LUC vector following the manufacture's recommendations (VT8124; Youbio Biological Technology Co. Ltd, Beijing, China). The constructs were separately transferred into *Agrobacterium tumefaciens* strain GV3101-pSoup-p19 (ZC1407; ZOMANBIO) and infiltrated into *N. benthamiana* leaves. Luciferase signal strength and activities in leaves were determined as explained for the dual-luciferase reporter assays.

Statistical analysis

The SPSS v.24.0 software package (<https://www.ibm.com/support/pages/downloading-ibm-spss-statistics-24>) was used for statistical analysis. *T*-tests with 95% confidence limits were used to analyze the significance of differences in plant morphological data, where *, **, *** and ns indicate significant differences at $P < 0.05$; $P < 0.01$; $P < 0.001$; and not significant, respectively. For multiple comparisons, significant differences were determined using one-way analysis of variance (ANOVA) and Duncan's multiple range tests, with different lowercase letters indicating significant differences at $P < 0.05$. The software GRAPHPAD PRISM 7 was used for plotting.

Results

Effects of *Q* on plant architecture

The *Q*-OE and *Q*-KO lines were used to clarify *Q* functions in modulating plant architecture. The *Q*-KO lines had slender plant stature with increased plant height and reduced stem thickness compared with the negative control Fielder, while *Q* OE significantly reduced plant height and increased the thickness of all main stem internodes (Figs 1a–d, S1A–D). Notably, *Q* KO reduced plant height uniformity (Fig. 1a,e). The *Q*-OE lines had a significantly increased spike width but a significantly reduced spike length, whereas *Q* KO significantly reduced spike width but had little effect on spike length (Figs 1f,g, S1E,F). *Q* KO also conferred shorter awn length (Fig. 1h). Leaf size and angle were significantly reduced in *Q*-KO lines and increased in *Q*-OE lines (Figs 1b,i–l, S1B,G–I). Tiller angle was obviously increased in *Q*-KO lines, but *Q* OE also significantly increased tiller angle, indicating that the domesticated *Q* allele (i.e. 5A*Q*) in wild-type (WT) lines (Fielder and CB037) could improve plant structure compactness in different genetic backgrounds (Figs 1m, S1J). *Q* KO greatly increased total tiller number and ineffective

tiller number per plant and consequently had little effect on the ear-bearing rate. Accordingly, effective tiller (spike) number per plant in *Q*-KO lines was enhanced compared with that in Fielder (Figs 1n–p, S1K–N).

Micromorphological and dynamic analysis of *Q* in modulating plant height, stem thickness, leaf size, and tiller number

To further clarify the regulatory mechanism of *Q* modulating plant architecture, we imaged micromorphological shape and dynamic developmental changes in target tissues. Histochemical staining showed that *Q* KO significantly increased cell length but reduced cell width and cavity diameter in stem internodes, indicating that *Q* reduced plant height and increased stem thickness by repressing cell aspect ratio and enhancing cavity diameter (Fig. 2a–d). However, *Q* had little effect on stem wall thickness (Fig. 2e). Given that cell staining by solid green dye is an indicator of major cell wall components, and the color intensity of stem cells differed between *Q*-KO lines and Fielder, we quantified the cellulose and lignin contents in stems and found that the *Q*-KO lines had higher cellulose contents but lower lignin than Fielder (Fig. 2f,g). We next investigated the cell size in flag leaf epidermis and observed that flag leaf cell length and width in *Q*-KO lines were significantly reduced compared with those in Fielder (Fig. 2h–j). *Q* KO also reduced leaf thickness (Fig. 2k). These results revealed that *Q* promoted flag leaf size by enhancing cell size. Considering the large effects of *Q* on tiller number, we investigated the dynamic development of tillers in *Q*-KO lines and Fielder. *Q* KO conferred more tiller buds and faster outgrowth of main tillers (Fig. 2l; labeled by blue arrows) than Fielder, indicating that *Q* is a negative regulator of tiller initiation. Conversely, secondary tillers (Fig. 2l; labeled by red arrows) in *Q*-KO lines grew more slowly than those in Fielder, hence accounting for *Q* contribution to plant uniformity.

Impact of *Q* on lodging resistance and yield potential

Since *Q* had significant effects on cellulose and lignin content in stem internodes, we compared the mechanical strength of *Q*-KO lines and Fielder. *Q* KO enhanced resistance to stem fracture (Fig. 3a). In addition, *Q*-KO lines had higher stem stiffness than Fielder (Fig. 3b). The field trial also validated that *Q*-KO lines had better lodging resistance than Fielder (Fig. S2A). These results showed that *Q* was a negative regulator of stem quality, unfavorable to lodging resistance. In fact, the enhanced expression of *Q* led to larger cavities in the internodes despite enhanced stem diameter (Figs 1b, 2d). Increased spike weight in Fielder was also negative to lodging resistance because it enhanced the height of plant's gravity center (Fig. S2B). Although *Q* potentially improved lodging resistance by reducing plant height, its effect on plant height reduction is minor, at least in Fielder (Fig. 1a,c).

In addition to reduced leaf size (Fig. 1b,k,l), flag leaves in *Q*-KO lines appeared to be lighter in color than those in Fielder (Fig. 1i). Measurement of Chl content and photosynthetic rate in

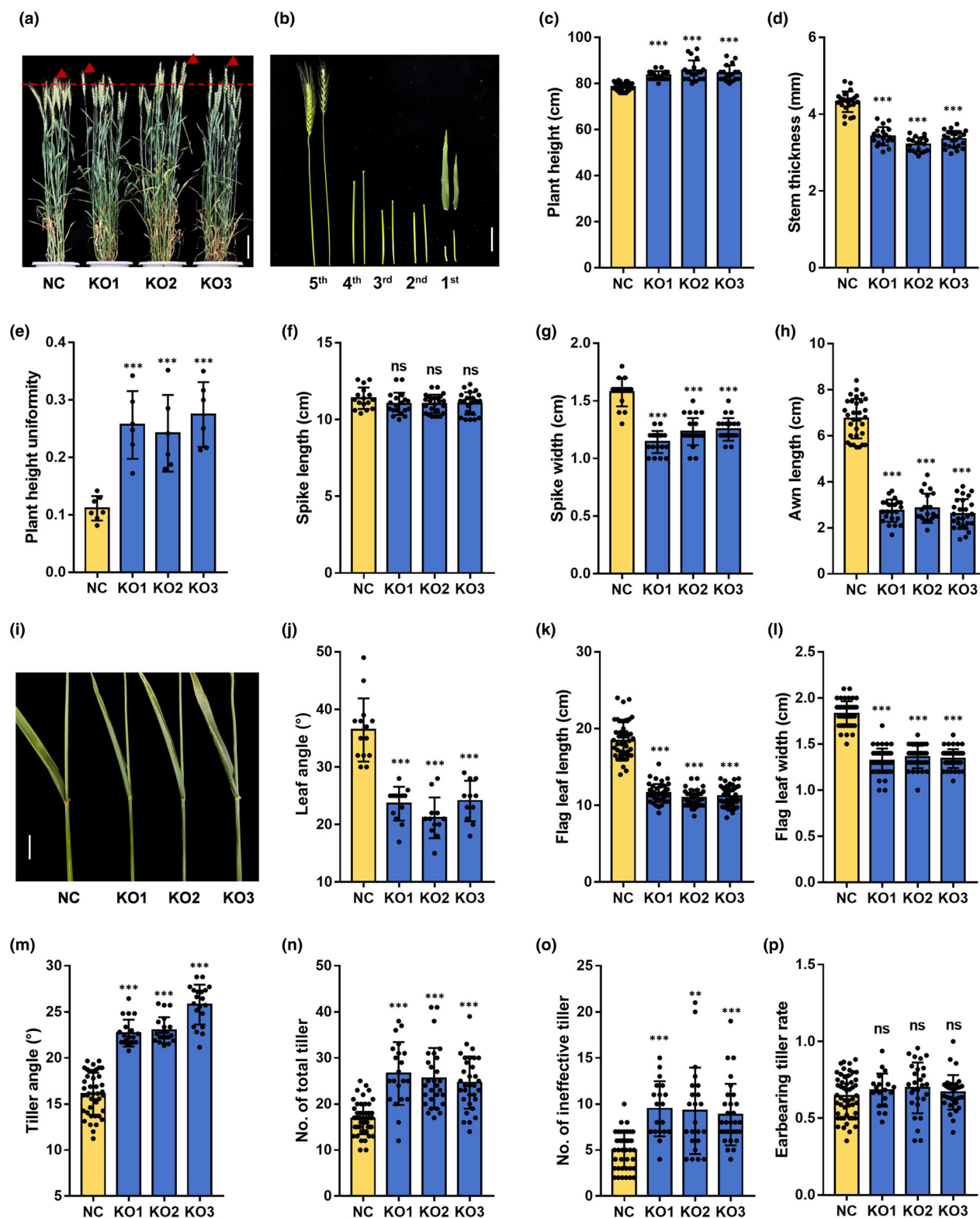


Fig. 1 Effects of Q on plant architecture. (a) Representative images of plant architecture of Q knockout lines (KO1–KO3) and negative control wheat cultivar Fielder (NC). Bar, 10 cm. (b) Close-up comparisons of the spikes, internodes, and flag leaves in main stems between a representative knockout line (KO) and NC. Bar, 5 cm. (c–h) Statistical comparisons of plant height (c), stem thickness (d), plant height uniformity (e), spike length (f), spike width (g), awn length (h) between KO1–KO3 and NC. *Note:* S/X , where X represents the mean of all tiller heights observed on individual plants and S denotes the SD, was used to quantify plant uniformity, and its resultant scores are inverse to plant uniformity. (i) Image comparisons of leaf angle between KO1–KO3 and NC. Bar, 3 cm. (j–p) Comparative analyses of leaf angle (j), flag leaf length (k), flag leaf width (l), tiller angle (m), number of total tiller (n), number of ineffective tiller (o), and ear-bearing tiller rate (p) between KO1–KO3 and NC. **, $P < 0.01$; ***, $P < 0.001$; ns, not significant.

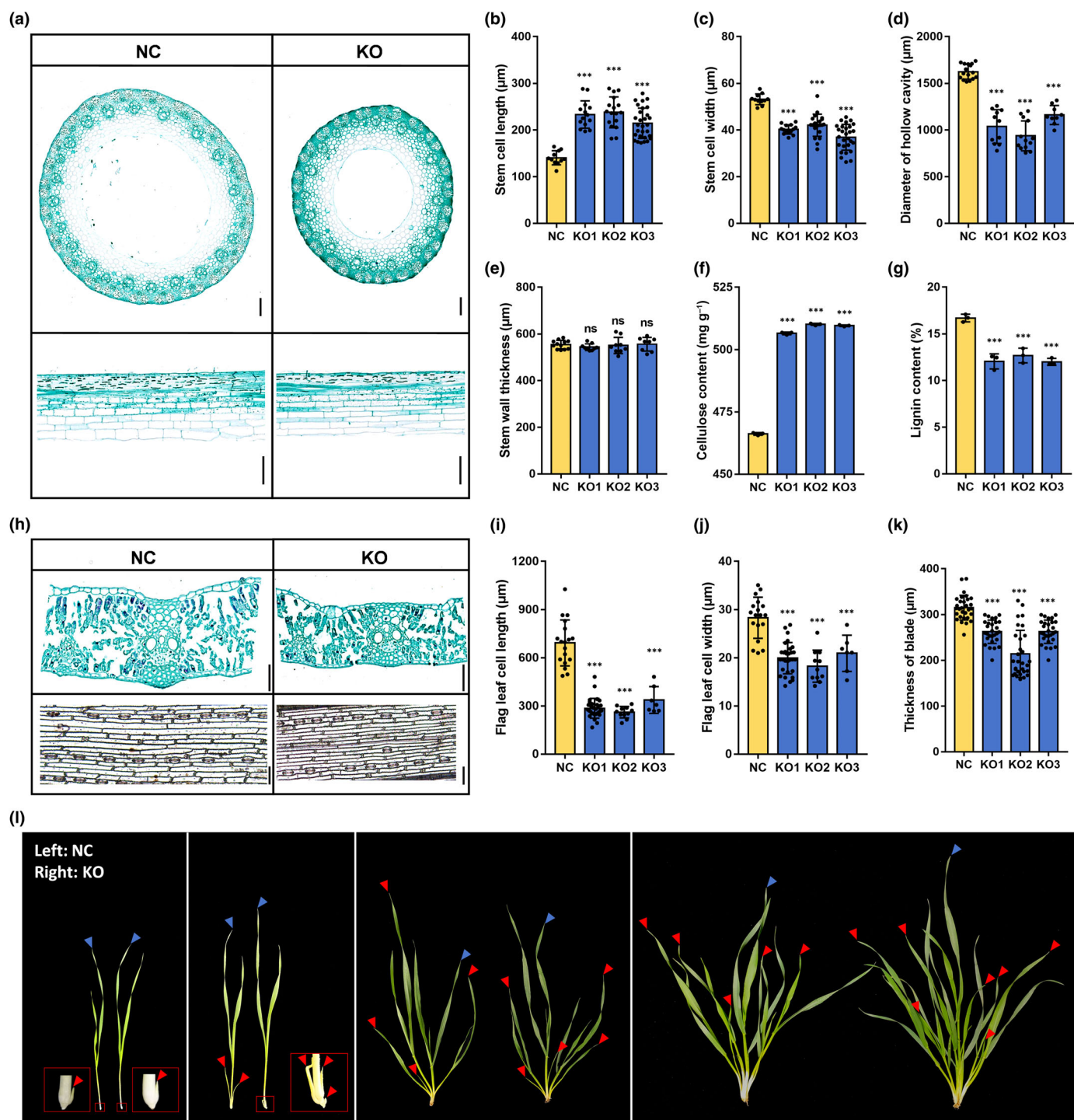


Fig. 2 Micromorphological and dynamic analyses of *Q* modulating plant height, stem thickness, leaf size, and tiller number. (a) Comparisons of solid green staining in transverse and longitudinal sections of stems between a representative *Q* knockout line (KO) and negative control wheat cultivar Fielder (NC). Bars, 200 μm . (b–g) Comparative analyses of stem cell length (b), stem cell width (c), diameter of hollow cavity (d), stem wall thickness (e), cellulose content (f), and lignin content (g) between *Q* knockout lines (KO1–KO3) and NC. (h) Comparisons of transverse and longitudinal sections of flag leaves between KO and NC. Bars, 100 μm . (i–k) Statistical comparisons of flag leaf cell length (i), flag leaf width (j) and thickness of blade (k) between KO1–KO3 and NC. (l) Comparisons of tiller initiation and outgrowth between KO and NC during the tillering stage. The red boxes are used to show the view for the close-up of tiny tillers. Main and secondary tillers are labeled by blue and red arrows, respectively. ***, $P < 0.001$; ns, not significant.

flag leaves showed that *Q* KO resulted in lower Chl content and reduced photosynthetic rate, suggesting that *Q* promotes photosynthetic capacity (Fig. 3d,e). *Q* is a negative regulator of spike

number, which is adverse to grain yield. Although *Q* KO increased spike number, most spikes in *Q*-KO lines contributed little to grain yield (Fig. 3c,f) because *Q* KO greatly reduced grain

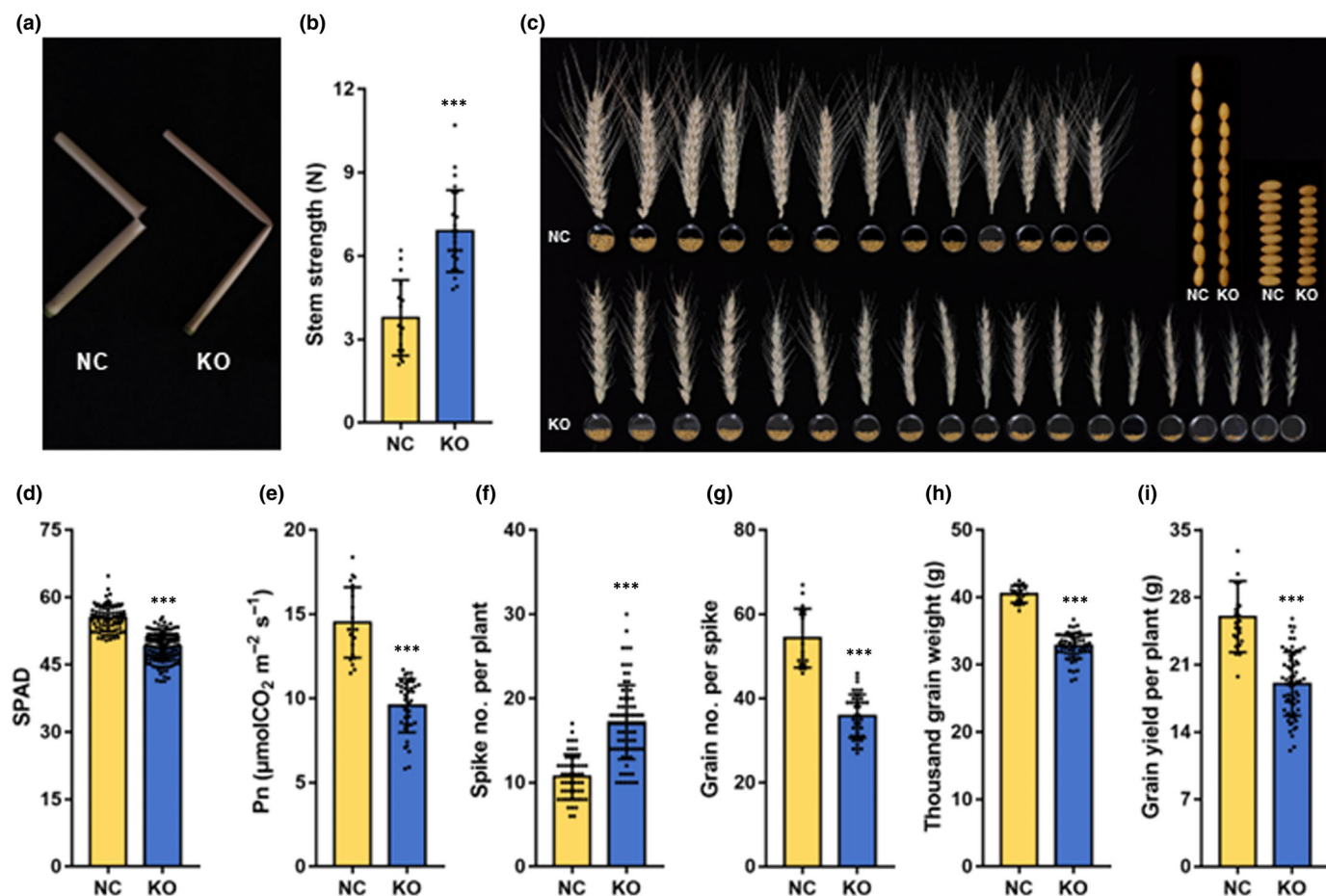


Fig. 3 Impact of *Q* on lodging resistance and yield potentials. (a) Physical properties of stem breakage of a representative *Q* knockout line (KO) and negative control wheat cultivar Fielder (NC). (b) Statistical comparisons of stem strength between KO and NC. (c) Image comparisons of spike number per plant, grain number per spike, and grain size between KO and NC. (d–i) Statistical comparisons of Chl content (SPAD) (d), photosynthetic rate (Pn) (e), spike number per plant (f), grain number per spike (g), thousand grain weight (h) and grain yield per plant (i) between KO and NC. ***, $P < 0.001$.

number per spike and thousand grain weight (Fig. 3g,h). Accordingly, *Q*-KO lines had significantly lower grain weight per plant than Fielder (Fig. 3i), indicating that *Q* is a positive regulator of grain yield.

Transcriptome and hormone quantitative analyses for *Q* gene modulating plant architecture

Transcriptome analysis, which detects DEGs in key spatial-temporal windows, is an effective way to uncover regulatory pathways or networks underpinning genes of interest. To identify the downstream genes of *Q*, we compared the transcriptome profiles of *Q*-KO lines and Fielder. As described above, *Q* affects stem, tiller, leaf, and spike morphogenesis. Considering that the machinery of *Q* modulating spike traits has been uncovered (Liu *et al.*, 2018; Song *et al.*, 2019), we focused on the dissection of its regulatory mechanisms underlying stem, tiller, and leaf development using transcriptome analysis.

Plant height and stem quality Since the pedicel is the most determinant stem internode for *Q* in modulating plant height

(Fig. 1b), the transcriptome sequencing of stems at ZGS 49 (late jointing) was used to mine downstream genes. In total, 1615 and 5995 DEGs were upregulated and downregulated by *Q* (Table S2). Quite a few DEGs were homologs of *OsMADS58* (Shen *et al.*, 2022), *expansins* (reviewed in Marowa *et al.*, 2016), *Os4CL3* (Gui *et al.*, 2011), *Os4CL4* (S. Liu *et al.*, 2020), *OsARF12* (Qi *et al.*, 2012), and *ZjHCT4* (Dong *et al.*, 2022), reported as promoters of plant height (Fig. 4a; Table S2). *Q* downregulated homologs of *MADS58*, *expansins*, *4CL3*, *4CL4*, and *HCT4*, consistent with the negative effects of *Q* on plant height. Strikingly, *Q* upregulated *OsARF12* orthologs *TaARF12-2B* and *TaARF12-2D*. A recent report showed that *TaARF12* was a promoter of plant height and a repressor of stem thickness (Kong *et al.*, 2023). *Q* also significantly affected both traits (Fig. 1c,d). Thus, *TaARF12* was a key downstream target of *Q* in modulating plant morphogenesis. However, *TaARF12* was counteractive to *Q* effects on plant height and stem thickness.

Q has large effects on stem strength. Lignin and cellulose are major cell wall components and determine stem mechanical properties. The homologs of *Os4CL3* (Gui *et al.*, 2011), *Os4CL4* (S. Liu *et al.*, 2020) and *ZjHCT4* (Dong *et al.*, 2022) that are

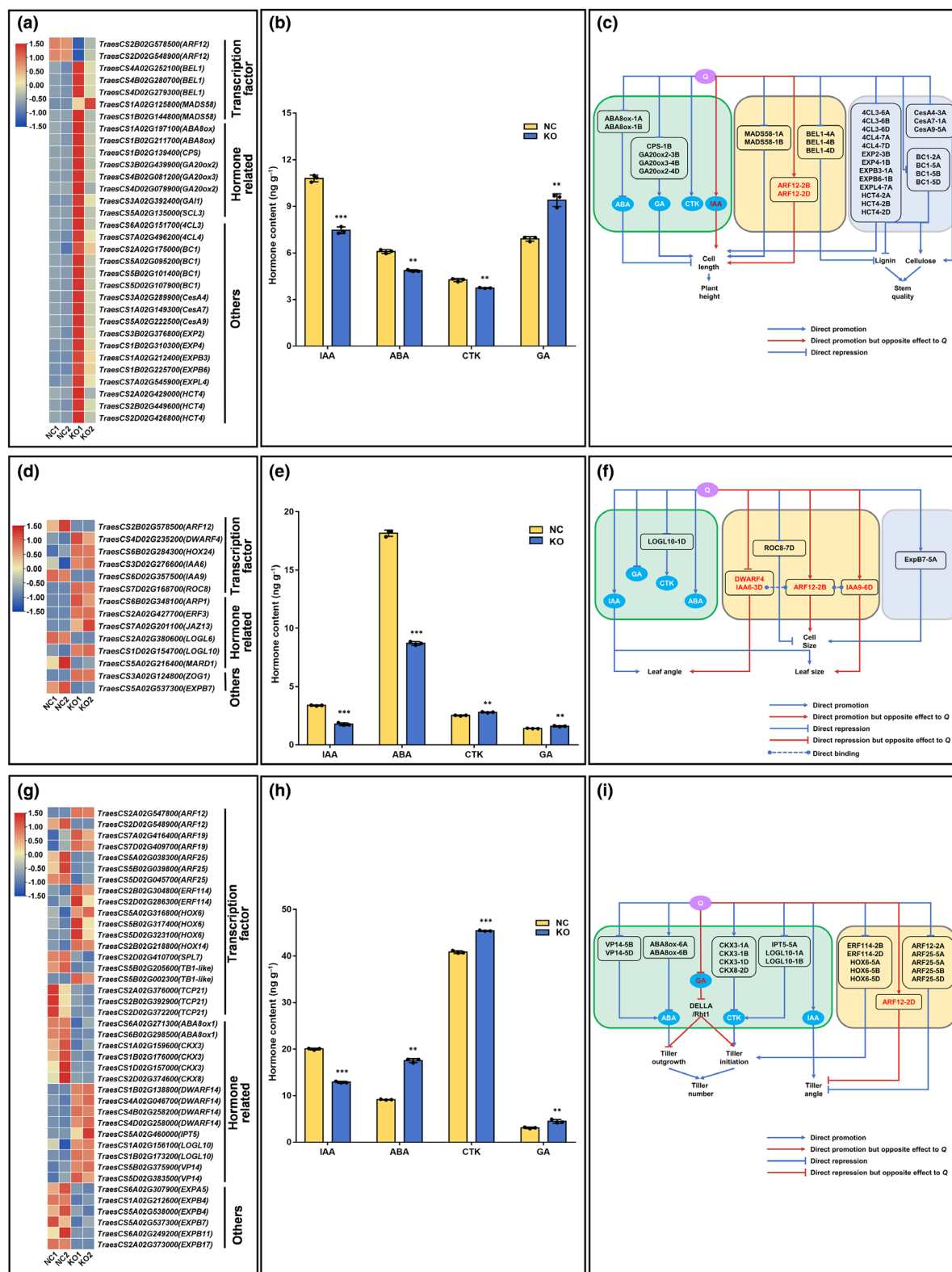


Fig. 4 Quantitative analyses of transcriptome and hormones for Q modulating plant architecture traits. Putative key differentially expressed genes in stem internodes (a), flag leaves (d) and tillers (g) between Q knockout lines (KO1–KO2) and wheat cultivar Fielder (negative controls: NC1–NC2). Quantitative comparisons of hormones in stem internodes (b), flag leaves (e), and tillers (h) between KO and NC. IAA, indole-3-acetic acid; ABA, abscisic acid; CTK, cytokinin; GA, gibberellin. Proposed regulatory models underpinning Q modulating stem internodes (c), flag leaves (f), and tillers (i). Genes or hormones with opposite effect to Q are also shown in red; the prefix 'Ta' in gene names is omitted. **, $P < 0.01$; ***, $P < 0.001$.

involved in lignin and/or cellulose biosynthesis were regulated by *Q*; thus, they probably modulated stem strength in wheat. A few homologs of cellulose synthases, including *OsCslE6*, *OsCslF2*, *OsCslF8*, *OsCesA4*, *OsCesA7*, and *OsCesA9*, were also differentially expressed between *Q*-KO lines and Fielder (Fig. 4a; Ye *et al.*, 2021). In rice, *BRITTLE CULM1 (BC1)* increased culm mechanical strength via increasing cellulose content but reducing lignin abundance (Li *et al.*, 2003). Four homologs of *BC1* were downregulated by *Q*. *BEL1*-like genes *SH5*, *KANT7*, and *BP* (Yoon *et al.*, 2015) were involved in regulating lignin biosynthesis, and their homologs *TaBEL1-4A*, *TaBEL-4B*, and *TaBEL-4D* were differentially expressed between *Q*-KO lines and Fielder. These results indicated that *Q* was a key modulator of stem strength by controlling lignin and cellulose biosynthesis.

In addition to DEGs that function in modulating plant morphogenesis and stem quality, many genes related to hormones, such as *ABA oxidases*, *SCL3* (Ito & Fukazawa, 2021), *CPS* (Zhang *et al.*, 2020) and *GA 20-oxidases*, were regulated by *Q*. Quantitative analyses of hormones in developing pedicels indicated that all tested hormones differed significantly in abundance between *Q*-KO lines and Fielder (Fig. 4b), suggesting that *Q* regulated stem morphogenesis by controlling the homeostasis of multiple hormones (Fig. 4b). Accordingly, we made a regulatory module of *Q* in modulating plant height and stem quality by integrating transcriptome and hormone quantitative analyses (Fig. 4c; Table S3).

Leaf size and angle We detected 2366 (1175 upregulated/1191 downregulated) DEGs in flag leaves between *Q*-KO lines and Fielder at ZGS 37 (Table S4). A few DEGs were homologs of genes involved in leaf development, such as *ROC8*, *DWARF4*, *expansin*, and *ARF12*. *ROC8* (Sun *et al.*, 2020) is a repressor of leaf size and their homologs are downregulated by *Q* (Fig. 4d). Expansins regulate cell size by catalyzing looseness of plant cell walls (Marowa *et al.*, 2016) and concomitantly promote leaf size (Cho & Cosgrove, 2000; Marowa *et al.*, 2020). *Q* upregulated an *expansin* gene *EXPB7-5A*, consistent with its promoting effect on leaf cell size (Fig. 4d). *OsARF12* was a promoting factor of leaf size, whereas *TaARF12* genes were validated as negative regulators of leaf size (Qi *et al.*, 2012; Kong *et al.*, 2023). Strikingly, *Q* upregulated *TaARF12-2D*, which is opposite to the *Q* effect on leaf size (Fig. 4d; Kong *et al.*, 2023). In addition to *ARF12* homologs, some auxin-related genes, such as *IAA6* and *IAA9*, were also differentially expressed between *Q*-KO lines and Fielder. In rice, *OsIAA6* is a promoter of leaf inclination (Xing *et al.*, 2022). However, *Q* downregulated *TaIAA6-3D*, contradictory with its positive effect on leaf angle (Figs 1i,j, 4d). *IAA9* in tomato is a repressor of leaf size (Rahmat *et al.*, 2023), but *Q* upregulated the homolog of *IAA9*, contrary to *Q* function in promoting leaf growth. Obviously, auxin-related DEGs play antagonistic roles in *Q* modulating leaf morphogenesis. An *OsDWARF4* mutant *osdwarf4-1* confers erect leaf in rice (Sakamoto *et al.*, 2006). *Q* repressed an *OsDWARF4* homolog, contrary to the *Q* effect on leaf angle (Fig. 1i,j).

In addition to IAA-related genes, many DEGs involving other hormones, such as *ABA-regulated RNA-binding Protein 1 (ARPI)*,

Mediator of ABA-regulated Dormancy1 (MARD1), *OsJAZ13*, *AtERF3*, *LOGL6*, *LOGL10*, and *AtZOG1* were detected between *Q*-KO lines and Fielder (Fig. 4d; Table S4). Quantitative analysis of hormone confirmed that *Q* had large effects on the abundance of all tested hormones in leaves, although we did not detect DEGs related to the metabolism of hormones (except CTK) between *Q*-KO lines and Fielder (Fig. 4e; Tables S3, S4). A regulatory module underpinning *Q* regulation of leaf morphogenesis was built (Fig. 4f).

Tiller number and angle A large number of DEGs (20724) were detected in tillers at ZGS 26 between *Q*-KO lines and Fielder, suggesting that almost all pathways involved in tillering were affected by *Q* (Table S5). *Q* regulated homologs of many transcription factors, including *ERF114*, *HOX6*, *HOX14*, *SPL7*, *TB1*, *TCP21*, and *ARFs* (*ARF12* and *ARF25*) that modulate tillering or branching (Fig. 4g). *AtERF114* and *OsHOX6* were identified as promoters of shoot branching or tiller number (Mehrnia *et al.*, 2013; Rahmawati *et al.*, 2019) and their homologs were downregulated by *Q*, consistent with the negative effect of *Q* on tiller number (Fig. 1n). By contrast, *HOX14* repressed tillering in rice (Shao *et al.*, 2018) and its homolog *TaHOX14-2B* was downregulated by *Q*. *OsSPL7* repressed tiller number (Dai *et al.*, 2018) and its homolog *TaSPL7-2D* was upregulated by *Q*, concordant with the repressive effect of *Q* on tillering. *TB1* is a key repressor of tiller formation in wheat (Dixon *et al.*, 2018). *Q* downregulated *TaTB1-5B1* but upregulated *TaTB1-5B2*. *OsTCP21* is a promoter of tiller number (Wang *et al.*, 2021), and its homologs were upregulated by *Q*. Transgenic rice plants over-expressing *miR167* had substantially decreased *OsARF12*, *OsARF17*, and *OsARF25* transcripts, and concomitantly had reduced tiller number (Liu *et al.*, 2012). However, mutations in each of the ARF genes conferred larger tiller angle and had little effect on tiller number in rice (Li *et al.*, 2020). Likewise, *taarf12* mutation promoted tiller angle and hardly affected tillering (Kong *et al.*, 2023). *Q* upregulated *TaARF12-2D*, consistent with its effect on tiller angle in *Q*-KO lines, and reversed to that in *Q*-OE lines (Figs 1m, S1j).

A few hormones, such as ABA, GA, IAA, CTK, and strigolactone, were reported to regulate tillering in rice, and some related genes in wheat have also been validated to regulate tillering (Shang *et al.*, 2021; Dong *et al.*, 2023; Yan *et al.*, 2023). Many genes affecting metabolism of hormones, such as ABA (*ABAox8* and *VP14*), CTK (*LOGL10*, *CKX3*, *CKX8*, and *IPT5*) and strigolactone (*DWARF14*) were differentially expressed between *Q*-KO lines and Fielder (Fig. 4g). *DWARF14 (D14)* repressed tiller bud occurrence and outgrowth in rice (Arite *et al.*, 2009). In addition, the wheat homolog *TaD14-4D* was associated with tiller number (Liu *et al.*, 2021). Homologs of *D14* were downregulated by *Q*, contrary to the negative effect of *Q* on tiller number. We further quantified the contents of hormones and found that all tested hormones had significantly different abundance in tillers between *Q*-KO lines and Fielder, indicating that multiple hormone homeostasis modulated tiller initiation and outgrowth (Fig. 4h; Table S3). We constructed a regulatory network underpinning *Q* modulating tillering (Fig. 4i).

Confirmation of Q interplay with *TaARF12*

TaARF12 was identified as a key regulator of plant architecture via IAA and GA homeostasis (Kong *et al.*, 2023). In the present study, *TaARF12-2B* and *TaARF12-2D* functioned as downstream genes of *Q*. Expression pattern analysis showed that *Q* and *TaARF12* had high expression levels in stems, leaves, and spikes, suggesting that they have overlapping spatio-temporal windows in modulating plant morphogenesis (Fig. 5a). In addition, like *Q*, *TaARF12* had a significant effect on multiple hormone homeostasis in stem internodes and flag leaves (Fig. 5b,c; Table S6). Y1H assays showed that *Q* could directly bind to the promoters of *TaARF12* genes. However, the region –400 to –150 upstream of the *TaARF12-2B* and *TaARF12-2D* start codons had the strongest affinity with *Q*, whereas the 150-bp region upstream of the start codon of *TaARF12-2A* harbored predominant binding sites of *Q* (Figs 5d,g, S3A). In addition, sequence alignment and motif analysis showed that there was a large difference in *cis*-acting element patterns of the promoters between *TaARF12-2A* and *TaARF12-2B* or *TaARF12-2D*, accounting for their differential expression patterns in response to *Q* (Fig. S3D,E). Tobacco transient expression assays further validated that *Q* promoted the expression of *TaARF12-2B* and *TaARF12-2D*, but repressed *TaARF12-2A* expression (Figs 5e,h, S3B). These results were also confirmed by enzymic activation assays (Figs 5f,i, S3C).

Genetic effects of allelic variations of *Q* and *TaARF12*

Since both *Q* and *TaARF12* had large effects on major agronomic traits, such as plant height, grain yield, and yield components (Kong *et al.*, 2023), favorable alleles were investigated for possible application in wheat breeding. Polymorphic sites in the genome regions spanning from 1.8-kb upstream and 1.5-kb downstream of their ORFs were retrieved and analyzed using genome resequencing databases in Wheat-SnpHub (http://wheat.cau.edu.cn/Wheat_SnpHub_Portal/). Variations causing missense mutations, premature stops, frameshift, or splicing mutations in ORFs and close to transcription start sites or polyadenylation signal sites were used to define haplotypes. Insertion/deletion (InDel) polymorphisms in the regions flanking ORFs were also considered to define haplotypes.

Q on chromosome 5A had two polymorphic sites that defined three haplotypes, *Q-Hap1*, *Q-Hap2*, and *Q-Hap3* with frequencies 91.9, 2.7, and 5.4%, respectively (Fig. S4A; Table S7). The frequencies of *Q-Hap2* and *Q-Hap3* in a diverse panel, including 166 elite wheat cultivars, are too low to identify their genetic effects due to lack of statistical power. As an alternative approach, we used a recombinant inbred line population derived from the cross Zhongmai 175 and Lunxuan 987 with *Q-Hap1* and *Q-Hap2*, respectively, to conduct an analysis of genetic effects and detected no significant difference in agronomic traits between the two haplotypes (Fig. S4B; Table S8; Sun *et al.*, 2023). Considering that the polymorphic site to distinguish *Q-Hap3* from the others is in the 3' untranslated region and probably affects mRNA stability, we quantified the abundance of *Q* in contrasting

cultivars with *Q-Hap1* and *Q-Hap3*, respectively, using qPCR assays, but found no significant difference between the two groups (Fig. S4C). Notably, all cultivars in the tested population had the domesticated allele 5A*Q*, indicating that it had been fixed in modern wheat cultivars (Table S7; Simons *et al.*, 2006).

We likewise identified variations in *TaARF12* and detected a large number of polymorphic sites in *TaARF12-2A* and *TaARF12-2B*, but no variation in *TaARF12-2D*. Both *TaARF12-2A* and *TaARF12-2B* had three haplotypes (Tables S9, S10). Gene-specific competitive allele-specific PCR (KASP) markers were developed to distinguish contrasting haplotypes. Marker-trait association analysis of the natural population found no significant differences in plant architecture and yield traits except grain number per spike and flag leaf length among the three haplotypes of *TaARF12-2A* (Fig. S5A,B; Table S11; Li *et al.*, 2019). By contrast, *TaARF12-2B-Hap1* and *TaARF12-2B-Hap2* conferred a reduction in plant height, flag leaf length, and spike number m⁻², but an increase in flag leaf width, thousand grain weight, and grain yield compared with *TaARF12-2B-Hap3* (Fig. 6a,b; Table S12). Therefore, *TaARF12-2B-Hap1* and *TaARF12-2B-Hap2* are favorable haplotypes for wheat improvement due to their contribution to lodging resistance and yield gain. *TaARF12-2B-Hap1* and *TaARF12-2B-Hap2* had frequencies of 76.3 and 12.7%, respectively, suggesting that the former had been subjected to positive selection in wheat breeding. However, a single nucleotide polymorphism (SNP) chip-based genome-wide association study did not detect any locus for plant height on chromosome 2B (Li *et al.*, 2019). The SNPs defining *TaARF12-2B* haplotypes are not available in the SNP chips, probably accounting for the differences in the results of the association analyses between this study and Li *et al.* (2019). Likewise, we did not observe the significant genetic effect of *TaARF12-2B* haplotypes on plant height in another natural population either (A. Li *et al.*, 2022), suggesting that population difference can cause the discrepancy of genetic loci associated with plant height.

Identification and evolution of the functional variation site of *TaARF12-2B*

Considering significant differences in genetic effects between *TaARF12-2B-Hap1* and *TaARF12-2B-Hap3*, we compared the transcriptional activity driven by their promoters in the tobacco transient expression system. Fluorescence imaging showed that the two promoters generated obviously different luciferase (LUC) signals, which were confirmed by the enzymic activation assays and indicated that there were functional variation sites in the promoters of *TaARF12-2B-Hap1* and *TaARF12-2B-Hap3* (Fig. 6c–g). Although there were many variation sites between *TaARF12-2B-Hap1* and *TaARF12-2B-Hap2*, the two haplotypes showed little difference in genetic effects, suggesting the polymorphic sites were not functional (Fig. 6a,b). As such, we created a series of promoter mutants to identify causal variations (Fig. 6c). LUC imaging and enzymic activation measurement indicated that an InDel (C/–) at –33-bp upstream of the start codon was the functional variation between *TaARF12-2B-Hap1* and *TaARF12-2B-Hap3* (Fig. 6d–g).

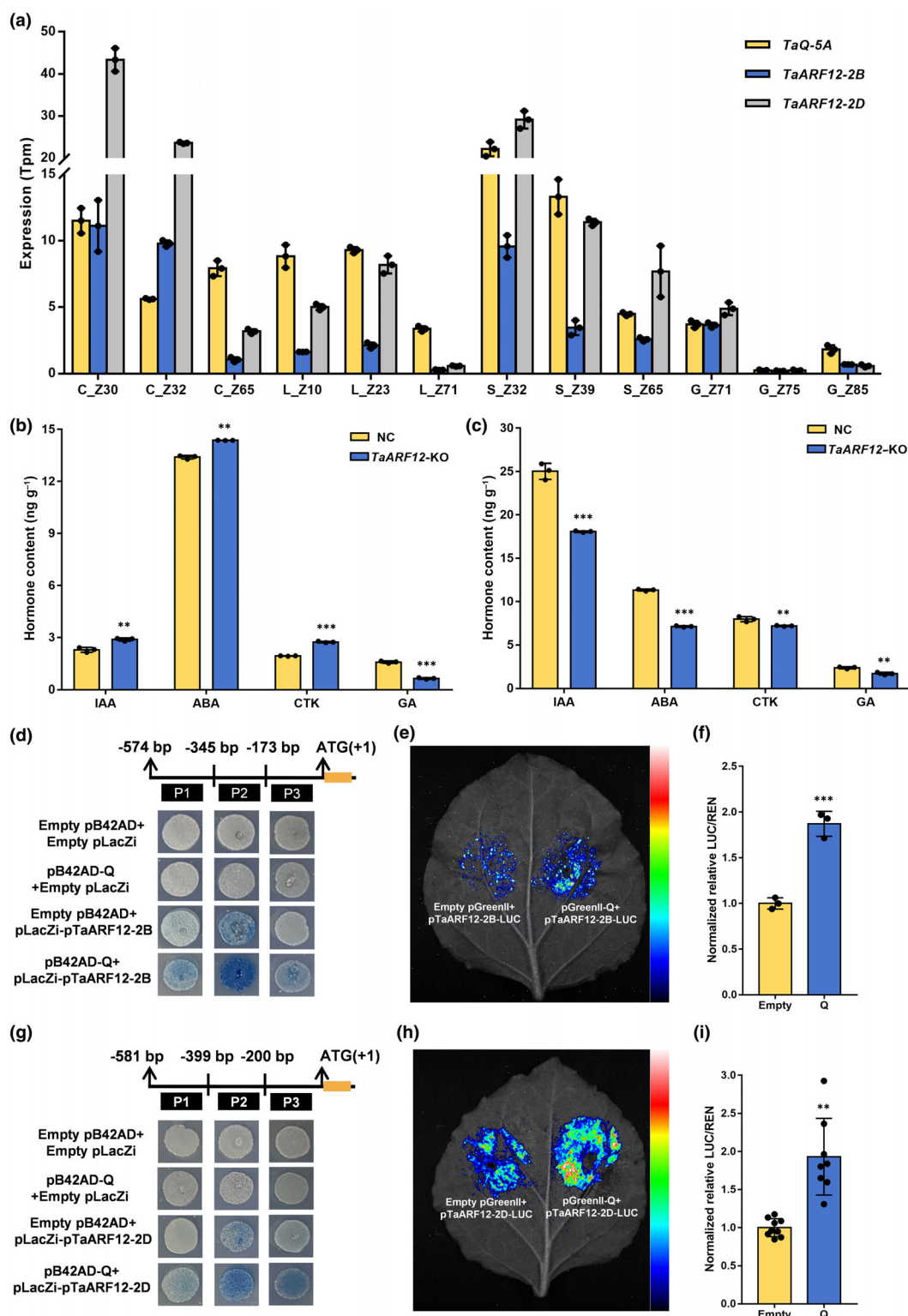


Fig. 5 Q encoded by *TaQ-5A* on chromosome 5A from Fielder binds directly to the promoters of *TaARF12-2B* and *TaARF12-2D*, and regulates their expression. (a) Expression patterns of Q and *TaARF12* in different spatio-temporal windows. C, culm; L, leaf; S, spike; G, grain; Z, Zadoks growth scale. Hormone quantitative comparisons of stem internodes (b) and flag leaves (c) between *TaARF12* knockout lines (*TaARF12-KO*) and negative controls (NC: wheat cultivar Fielder). IAA, indole-3-acetic acid; ABA, abscisic acid; CTK, cytokinin; GA, gibberellin. (d, g) Yeast one-hybrid assays identified the interaction between Q and different fragments (P1–P3) of the *TaARF12* promoters. (e, h) Dual-luciferase reporter assays validated Q effects on *TaARF12* expression in *N. benthamiana* leaves. (f, i) Normalized LUC/REN ratio based on enzymic activity measurements. Empty and Q in (f) represent Empty pGreenII + pTaARF12-2B-LUC and pGreenII-Q + pTaARF12-2B-LUC, respectively, in (e). Empty and Q in (i) represent Empty pGreenII + pTaARF12-2D-LUC and pGreenII-Q + pTaARF12-2D-LUC, respectively, in (h). **, $P < 0.01$; ***, $P < 0.001$.

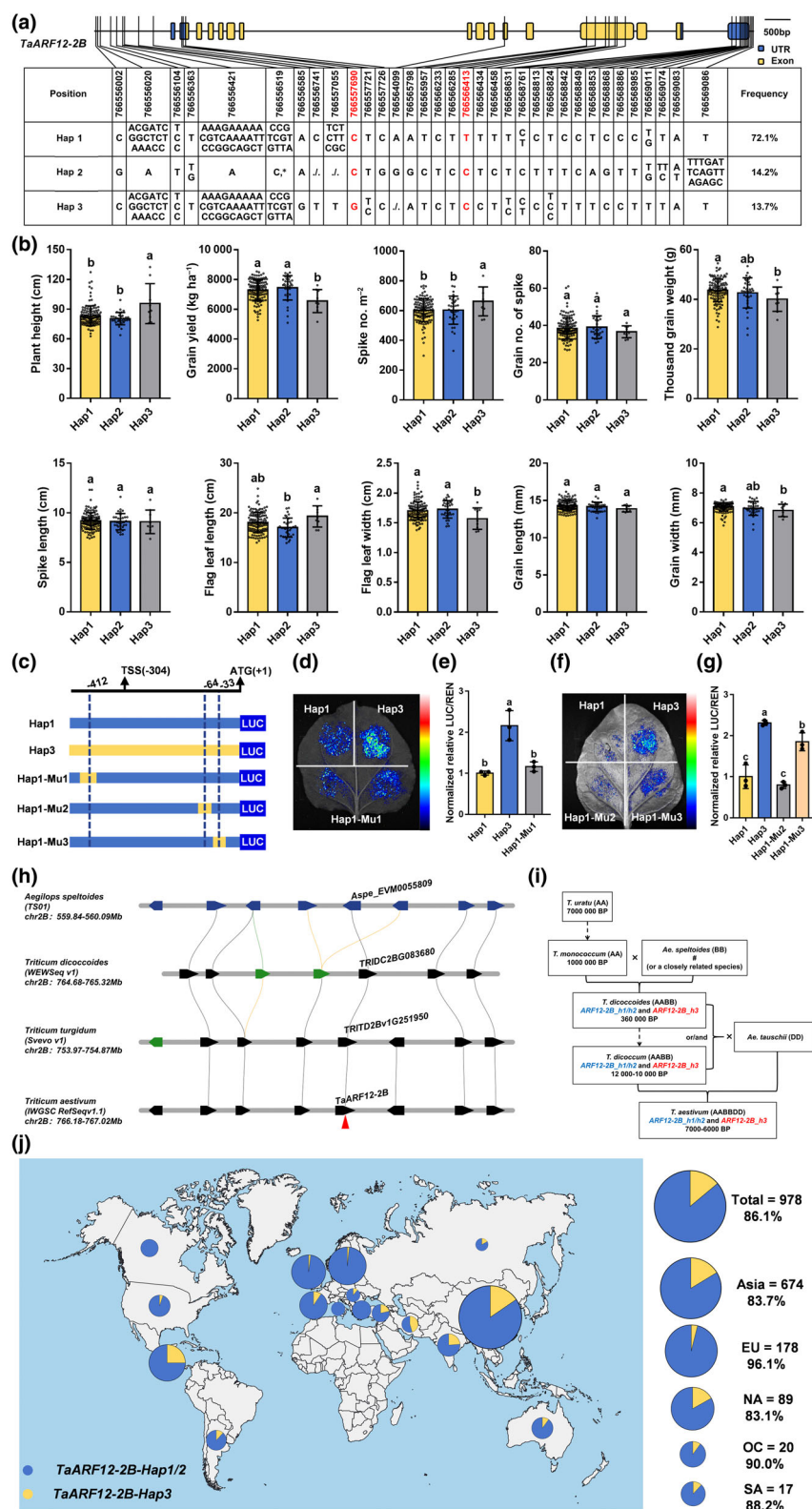


Fig. 6 Genetic effect, functional variation, and evolutionary trajectory of major haplotypes of *TaARF12-2B*. (a) *TaARF12-2B* haplotypes and their frequency distribution in a diverse panel of 166 wheat cultivars. The diagnostic markers were developed according to the polymorphic sites shown in red. (b) Genetic effects of major haplotypes in a diverse panel of 166 wheat cultivars. Different and same letters above the columns represent significant difference at $P < 0.05$ and nonsignificant difference, respectively. (c–g) Identification of the functional variation between *TaARF12-2B*-Hap1 and *TaARF12-2B*-Hap3. (c) Schematics of the vectors constructed for dual-luciferase reporter assays. LUC, firefly luciferase. (d, f) Transient expression activities driven by Hap1, Hap3, Hap1-Mu1, Hap1-Mu2, and Hap1-Mu3 in *N. benthamiana* leaves. Hap1 and Hap3 represent the promoters of *TaARF12-2B* haplotypes Hap1 and Hap3; Hap1-Mu1, Hap1-Mu2, and Hap1-Mu3 represent Hap1 promoter versions with different targeted mutations. TSS, transcription start site. (e, g) Normalized enzymatic activities of LUC/REN ratio. Different and same letters above the columns represent significant difference at $P < 0.05$ and nonsignificant difference, respectively. (h) Collinearity analysis of the *TaARF12-2B* locus across several *Triticeae* species, including *Ae. Speltoides*, *T. dicoccoides*, and *T. durum*. (i) Evolutionary origin of the favorable *TaARF12-2B*-Hap1 and Hap2, designated as *TaARF12-2B*-Hap1/2. Polyploidization and domesticated events for speciation of common wheat are represented as a flowchart. # indicates uncertainty about the donor of common wheat subgenome B. (j) Schematic of global distribution of *TaARF12-2B*-Hap1/2 in a world-wide wheat collection. Percentages in the pie chart indicate the proportion of *TaARF12-2B*-Hap1/2 in different continents. EU, Europe; NA, North America; OC, Oceania; SA, South America.

Wheat (*Triticum aestivum* L, AABBDD) is a hexaploid species formed by two polyploidization events (Pont *et al.*, 2019). Tetraploid wild emmer (*T. dicoccoides*, AABB) evolved from spontaneous chromosome doubling of a hybrid of an unknown extinct

or extant Sitopsis species and *T. urartu*. The second polyploidization event involved a hybrid of a domesticated tetraploid (*T. dicoccum*) and the D subgenome donor species *Ae. tauschii*. Recent genome assembly of chromosome-level genome sequences

of all five *Sitopsis* species, namely *Aegilops bicornis*, *Ae. longissima*, *Ae. searsii*, *Ae. sharonensis*, and *Ae. speltooides* reveals that the donor of the common wheat B subgenome is distinct, and most probably extinct (L. Li *et al.*, 2022). However, haplotype block analysis supported the idea that *Ae. speltooides* genome is closest to the wheat B subgenome (Avni *et al.*, 2022). Genomic synteny analyses showed that *TaARF12-2B* was orthologous to *Aspe_EVM0055809* in *Ae. speltooides* and *TRIDC2BG083680* in wild emmer (Fig. 6h). *TaARF12-2B* favorable haplotypes *TaARF12-2B-Hap1* and *TaARF12-2B-Hap2* had the same functional variation and were designated as *TaARF12-2B-Hap1/2*. We investigated *TaARF12-2B* allelic variations in 42 tetraploid (AABB) genotypes and found *TaARF12-2B-Hap1/2* in wild emmer (*T. dicoccoides*, 10/22 accessions), domesticated emmer (*T. dicoccum*, 7/9 accessions) and durum (*T. durum*, 11/11 accessions; Fig. 6i; Table S13). These results showed *TaARF12-2B-Hap1/2* first appeared in wild emmer and thus were ancient natural alleles (Fig. 6i).

To determine the distribution of *TaARF12-2B-Hap1/2*, we investigated 978 wheat accessions from various regions worldwide (Table S14). Genotyping analysis showed that c. 86.1% of accessions harbored *TaARF12-2B-Hap1/2*. The *TaARF12-2B-Hap1/2* has the highest frequency (96.1%) in wheat lines from Europe and the lowest frequency (83.1%) in lines from North America (Fig. 6j; Table S15). Overall, these results suggested that *TaARF12-2B-Hap1/2* had been positively selected in wheat breeding programs worldwide.

Discussion

Q contributes to ideal plant architecture and yield potential in wheat breeding

Q as the most important domestication gene controls free threshability of grains. Previous research focused on phenotypic and mechanistic dissection of Q function in spike development. Here, we systematically dissected the various functions of Q in modulating plant height, tiller number and angle, leaf size and angle, and spike size using Q-KO and Q-OE lines in different genetic backgrounds. The 5AQ in WT lines not only reduced plant height but also increased stem thickness compared with Q-KO lines, suggesting that Q is positive for enhancing lodging resistance in terms of stem morphology (Fig. 1a–d). 5AQ also conferred a moderate increase in flag leaf angle and an appropriate reduction in tiller number and angle, favorable to ventilation and light penetration of the wheat canopy (Fig. 1i,j,m–o). Since ineffective tiller production is a waste of metabolites and energy (Feng *et al.*, 2021), Q acts as a negative regulator of ineffective tillers and consequently contributes to more efficient plant morphogenesis. In addition, Q increases plant uniformity, flag leaf size, Chl content and photosynthetic efficiency, helpful to improve wheat productivity (Figs 1e,k,l, 3d,e,i; Yang *et al.*, 2024). In fact, the domesticated Q reduced SN but greatly promoted grain number per spike, thousand grain weight, and grain yield (Fig. 3f–i). The ideal plant architecture proposed in rice includes thick stems, upward sloping leaves, fewer ineffective

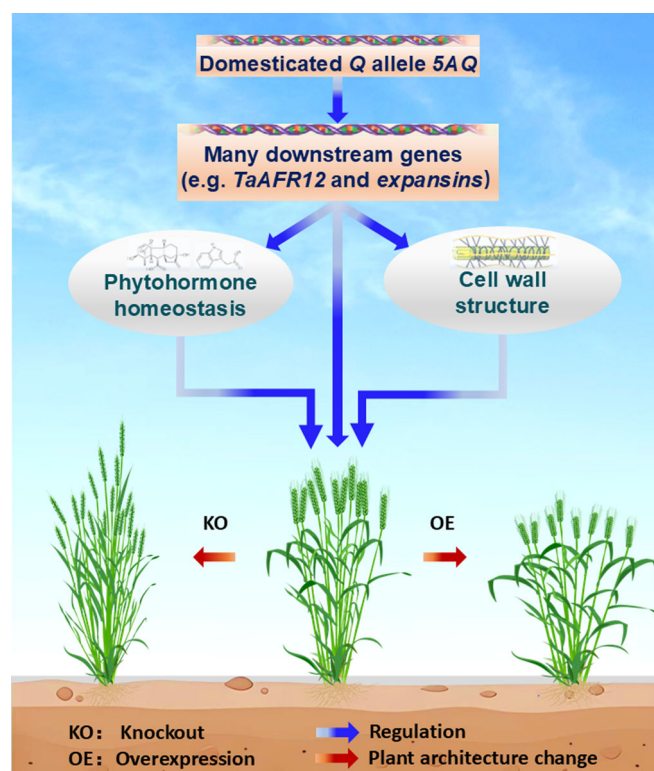


Fig. 7 Simplified module underpinning the domesticated Q allele (5AQ) contributing to wheat ideal plant architecture largely through modulating hormone homeostasis and cell wall skeleton. The wheat ideal plant architecture is characterized by moderately reduced plant height, tiller angle, flag leaf angle, and spike number, minimized ineffective tiller number, but appropriately enhanced stem thickness, leaf size, and spike size with more kernels, according to the counterpart features in rice (Jiao *et al.*, 2010). Most importantly, the wheat ideal plant architecture enables optimization of yield components and maximization of grain yield.

tillers, larger panicles, and more grains per spike (Jiao *et al.*, 2010). Thus, Q is a key promoting regulator to optimize plant architecture. The 5AQ confers stable transcripts (Simons *et al.*, 2006) and robust function in homodimerization (Liu *et al.*, 2018) and endows plant ideal architecture and yield formation via orchestrating yield components, accounting for why they have been largely fixed in modern wheat cultivars. We proposed a module of the domesticated Q contributing to ideal plant architecture traits (Fig. 7). However, Q also has adverse effects on stem quality (Fig. 3a,b). Although 5AQ could enhance lodging resistance by reducing plant height and increasing culm thickness, it could impair lodging resistance by reducing culm strength and increasing culm hollowness and spike weight (Figs 1c,d, 2d, 3a,b, S2A,B). Since the domesticated Q allele is prevalent in modern wheat cultivars, great effort should be exerted to enhance culm quality. The 5AQ in the WT lines reduces plant height to a very limited extent compared with its KO (Fig. 1a–c). 5AQ encodes an AP2 transcription factor and its homologs, such as *AP2L2*, have a similar function in modulating plant height (Debernardi *et al.*, 2020; Zhang *et al.*, 2025), thus *AP2L2* genes may have a compensation function for 5AQ KO. Transcriptome analysis showed that *AP2L2* genes in Q-KO lines were upregulated

compared with those in WT lines (Table S16). So far, several dwarfing genes, such as *Rht8*, *Rht12b* and *Rht24b* that reduce plant height without negative effects on yield have been identified. The 5A*Q* pyramiding with such dwarfing genes is an alternative approach for synergistic improvement of yield stability and potentials.

Functional dissection of *Q* provides many cues to uncover the regulatory mechanism underlying plant morphogenesis and yield formation

In this study, we not only comprehensively dissected *Q* effects on plant architecture traits but also parsed the underlying mechanism through micromorphology, dynamic imaging, transcriptome, and quantitative metabolite assays. Many genes were differentially expressed in all tested tissues between *Q*-KO lines and Fielder. More than 20 000 DEGs were detected in tiller nodes, suggesting that most active genes in tillers were influenced by *Q*. Hormones are important regulators involving almost all processes of plant growth and development. Many genes related to hormone metabolism and signal transduction in the tested tissues were regulated by *Q* (Fig. 4a,d,g). Quantitative analysis of hormones also verified that *Q* significantly affected the abundance of all tested major hormones in given tissues (Fig. 4b,e,h). *Q* KO led to distinct abundances and even opposite distribution patterns of some hormones (e.g. ABA and CTK) in different tissues, suggesting that *Q* controls plant architecture via regulating the homeostasis of multiple hormones (Fig. 4b,c,e,f,h,i). *Q* also had great effects on the plasticity of gene expression in modulating multiple traits. Some genes had diverse, even reverse expression patterns in response to *Q* in different spatio-temporal windows (Fig. 4a,d,g). *TaARF12* genes were validated as important regulators of plant architecture and acted as promoters of plant height and leaf size (Kong *et al.*, 2023). *Q* caused different expression patterns of *TaARF12-2A*, *TaARF12-2B*, and *TaARF12-2D* in tested tissues (Fig. 5e,f,h,i, S3B,C). We confirmed that *Q* directly binds to the promoters of *TaARF12* genes and regulates their expression. However, *TaARF12-2B* and *TaARF12-2D* were upregulated by *Q*, which was antagonistic to *Q* function in modulating plant architecture traits, such as plant height and leaf size, suggesting that *TaARF12* is a 'brake' component of *Q* modulating plant height. This result also showed the mechanical complexity underlying *Q* function in plant height control. In fact, like *Q*, functionally pleiotropic Green Revolution gene *Rht-B1b* also has some downstream genes causing negative feedback regulation (Xu *et al.*, 2023). For example, *TB1* genes in wheat repress tillering (Dixon *et al.*, 2018), whereas *Rht-B1b* OE improves tiller initiation but upregulates *TB1-like* genes. Likewise, *D14* in rice inhibits tillering and participates in the conversion of strigolactone to the bioactive form (Arite *et al.*, 2009), whereas its wheat homologs were upregulated by *Rht-B1b*. *OsYABBY4* is a negative regulator of plant height (Yang *et al.*, 2016), but one of its homologs was downregulated by *Rht-B1b*. *DWARF10* and *OsDWARF* also are positive regulators of plant height (Hong *et al.*, 2002; Arite *et al.*, 2007), whereas their homologs were upregulated by *Rht-B1b*. Overall, such components can trigger negative feedback regulatory loops of target traits, an important machinery

conferring the synergy and plasticity of crop growth and development. We further identified favorable alleles of *TaARF12-2B* and clarified the functional variation. A diagnostic marker was developed according to the functional variation to identify favorable alleles. These outcomes provide genetic resources and molecular tools for wheat breeding.

In addition to hormone-related genes, many genes involved in cellulose and lignin metabolism were regulated by *Q* (Tables S2, S4, S5). Histochemical staining and quantitative metabolite analyses confirmed that *Q* had large effects on lignin and cellulose contents. Since lignin and cellulose are the main components of the cell wall and maintain the cell cytoskeleton, *Q* plays a key role in modulating the structure and function of plant tissues and organs. Many differentially expressed *expansin* genes that can loosen the cell wall were also detected in tested tissues. Cellular imaging indicated that *Q* modulated cell size in stem internodes and leaves. The *brittle culm1* (*BC1*) genes modulate cell wall structure and are responsible for brittle rachis, another important domestication trait (Li *et al.*, 2003). *BC1* homologs were identified as downstream targets of *Q*, suggesting synchronization of spike threshability and shattering. In addition to protein-coding genes, quite a lot of noncoding RNA DEGs were also detected between *Q*-KO lines and Fielder in all test tissues (Table S17), suggesting the complex role of *Q* in modulating plant architecture.

Overall, *Q* is a versatile master regulator that controls the network underpinning plant architecture largely by modulating multiple hormone homeostasis and cell wall skeleton (Fig. 7). These findings provide important entry points to uncover the molecular regulatory mechanism of plant morphogenesis and yield formation.

Acknowledgements

We are grateful to Prof. Robert McIntosh, Plant Breeding Institute, University of Sydney, for reviewing this manuscript. This work was supported by the National Key Research and Development Program of China (2022YFF1002904 and 2022YFD1201500), the Key International (Regional) Cooperative Research Programs (W2411025), the National Natural and Science Foundation of China (32472191), and Central Public-interest Scientific Institution Basal Research Fund (S2025QZ03).



Competing interests

None declared.

Author contributions

BYL, MJS, KW, YJB, YQC, JDL, XML, SYL, LNX, LLL, KJQ, YHC and RC performed the experiments and participated in field trials. SHC and BYL wrote the draft manuscript. SHC, ALL and ZHH designed the experiments. XCX, LM and XGY assisted in writing the manuscript.

ORCID

Shuanghe Cao  <https://orcid.org/0000-0002-2905-0728>
 Zhonghu He  <https://orcid.org/0000-0003-1384-3712>
 Aili Li  <https://orcid.org/0000-0001-9004-192X>
 Long Mao  <https://orcid.org/0000-0002-3377-4040>
 Ke Wang  <https://orcid.org/0000-0001-6776-4935>
 Xianchun Xia  <https://orcid.org/0000-0003-2071-197X>
 Xingguo Ye  <https://orcid.org/0000-0002-6616-2753>

Data availability

The data that support the findings of this study are available in Supporting Information Tables S1–S17.

References

- Aríte T, Iwata H, Ohshima K, Maekawa M, Nakajima M, Kojima M, Sakakibara H, Kyojuka J. 2007. DWARF10, an RMS1/MAX4/DAD1 ortholog, controls lateral bud outgrowth in rice. *The Plant Journal* 51: 1019–1029.
- Aríte T, Umehara M, Ishikawa S, Hanada A, Maekawa M, Yamaguchi S, Kyojuka J. 2009. d14, a strigolactone-insensitive mutant of rice, shows an accelerated outgrowth of tillers. *Plant & Cell Physiology* 50: 1416–1424.
- Avni R, Lux T, Minz-Dub A, Miller E, Sela H, Distelfeld A, Deek J, Yu G, Steuernagel B, Pozniak C *et al.* 2022. Genome sequences of three *Aegilops* species of the section *Sitopsis* reveal phylogenetic relationships and provide resources for wheat improvement. *The Plant Journal* 110: 179–192.
- Bian Y, Li L, Tian X, Xu D, Sun M, Li F, Xie L, Liu S, Liu B, Xia X *et al.* 2023. *Rht12b*, a widely used ancient allele of *TaGA2oxA13*, reduces plant height and enhances yield potential in wheat. *Theoretical and Applied Genetics* 136: 253.
- Chen C, Chen H, Zhang Y, Thomas H, Frank M, He Y, Xia R. 2020. TBtools: an integrative toolkit developed for interactive analyses of big biological data. *Molecular Plant* 13: 1194–1202.
- Cho H, Cosgrove D. 2000. Altered expression of expansin modulates leaf growth and pedicel abscission in *Arabidopsis thaliana*. *Proceedings of the National Academy of Sciences, USA* 97: 9783–9788.
- Dai Z, Wang J, Yang X, Lu H, Miao X, Shi Z. 2018. Modulation of plant architecture by the miR156f-OsSPL7-OsGH3.8 pathway in rice. *Journal of Experimental Botany* 69: 5117–5130.
- Debernardi J, Greenwood J, Jean Finnegan E, Jernstedt J, Dubcovsky J. 2020. APETALA 2-like genes *AP2L2* and *Q* specify lemma identity and axillary floral meristem development in wheat. *The Plant Journal* 101: 171–187.
- Debernardi J, Woods D, Li K, Li C, Dubcovsky J. 2022. MiR172-APETALA2-like genes integrate vernalization and plant age to control flowering time in wheat. *PLoS Genetics* 18: e1010157.
- Dixon L, Greenwood J, Bencivenga S, Zhang P, Cockram J, Mellers G, Ramm K, Cavanagh C, Swain S, Boden S. 2018. *TEOSINTE BRANCHED1* regulates inflorescence architecture and development in bread wheat (*Triticum aestivum*). *Plant Cell* 30: 563–581.
- Dong C, Zhang L, Zhang Q, Yang Y, Li D, Xie Z, Cui G, Chen Y, Wu L, Li Z *et al.* 2023. *Tiller Number1* encodes an ankyrin repeat protein that controls tillering in bread wheat. *Nature Communications* 14: 836.
- Dong D, Yang Z, Ma Y, Li S, Wang M, Li Y, Liu Z, Jia C, Han L, Chao Y. 2022. Expression of a hydroxycinnamoyl-CoA shikimate/quinate hydroxycinnamoyl transferase 4 gene from *Zoysia japonica* (*ZjHCT4*) causes excessive elongation and lignin composition changes in *Agrostis stolonifera*. *International Journal of Molecular Sciences* 23: 9500.
- Faris J, Fellers J, Brooks S, Gill B. 2003. A bacterial artificial chromosome contig spanning the major domestication locus *Q* in wheat and identification of a candidate gene. *Genetics* 164: 311–321.
- Feng Z, Q Z, Zhang Z, Zheng E, Yu J, Zheng Y. 2021. Effective tiller numbers, photosynthetic and yield response of rice (*Oryza sativa*) to shallow wet-dry irrigation water controlled at tillering stage in black soil area. *Agricultural Research* 10: 97–104.
- Förster S, Schumann E, Baumann M, Weber WE, Pillen K. 2013. Copy number variation of chromosome 5A and its association with *Q* gene expression, morphological aberrations, and agronomic performance of winter wheat cultivars. *Theoretical and Applied Genetics* 126: 3049–3063.
- Gui J, Shen J, Li L. 2011. Functional characterization of evolutionarily divergent 4-coumarate:coenzyme A ligases in rice. *Plant Physiology* 157: 574–586.
- Hong Z, Ueguchi-Tanaka M, Shimizu-Sato S, Inukai Y, Fujioka S, Shimada Y, Takatsuto S, Agetsuma M, Yoshida S, Watanabe Y *et al.* 2002. Loss-of-function of a rice brassinosteroid biosynthetic enzyme, C-6 oxidase, prevents the organized arrangement and polar elongation of cells in the leaves and stem. *The Plant Journal* 32: 495–508.
- International Wheat Genome Sequencing, C. 2014. A chromosome-based draft sequence of the hexaploid bread wheat (*Triticum aestivum*) genome. *Science* 345: 1251788.
- Ito T, Fukazawa J. 2021. SCARECROW-LIKE3 regulates the transcription of gibberellin-related genes by acting as a transcriptional co-repressor of GAI-ASSOCIATED FACTOR1. *Plant Molecular Biology* 105: 463–482.
- Jiao Y, Wang Y, Xue D, Wang J, Yan M, Liu G, Dong G, Zeng D, Lu Z, Zhu X *et al.* 2010. Regulation of *OsSPL14* by *OsmiR156* defines ideal plant architecture in rice. *Nature Genetics* 42: 541–544.
- Kline LM, Hayes DG, Womac AR, Labbé N. 2010. Simplified determination of lignin content in hard and soft woods via uv-spectrophotometric analysis of biomass dissolved in ionic liquids. *BioResources* 5: 1366–1383.
- Kong X, Wang F, Wang Z, Gao X, Geng S, Deng Z, Zhang S, Fu M, Cui D, Liu S *et al.* 2023. Grain yield improvement by genome editing of *TaARF12* that decoupled peduncle and rachis development trajectories via differential regulation of gibberellin signalling in wheat. *Plant Biotechnology Journal* 21: 1990–2001.
- Li A, Hao C, Wang Z, Geng S, Jia M, Wang F, Han X, Kong X, Yin L, Tao S *et al.* 2022. Wheat breeding history reveals synergistic selection of pleiotropic genomic sites for plant architecture and grain yield. *Molecular Plant* 15: 504–519.
- Li F, Wen W, Liu J, Zhang Y, Cao S, He Z, Rasheed A, Jin H, Zhang C, Yan J *et al.* 2019. Genetic architecture of grain yield in bread wheat based on genome-wide association studies. *BMC Plant Biology* 19: 168.
- Li L, Zhang Z, Wang Z, Li N, Sha Y, Wang X, Ding N, Li Y, Zhao J, Wu Y *et al.* 2022. Genome sequences of five *Sitopsis* species of *Aegilops* and the origin of polyploid wheat B subgenome. *Molecular Plant* 15: 488–503.
- Li Y, Li J, Chen Z, Wei Y, Qi Y, Wu C. 2020. OsmiR167a-targeted auxin response factors modulate tiller angle via fine-tuning auxin distribution in rice. *Plant Biotechnology Journal* 18: 2015–2026.
- Li Y, Qian Q, Zhou Y, Yan M, Sun L, Zhang M, Fu Z, Wang Y, Han B, Pang X *et al.* 2003. *BRITTLE CULM1*, which encodes a COBRA-like protein, affects the mechanical properties of rice plants. *Plant Cell* 15: 2020–2031.
- Lin R, Ding L, Casola C, Ripoll DR, Feschotte C, Wang H. 2007. Transposase-derived transcription factors regulate light signaling in *Arabidopsis*. *Science* 318: 1302–1305.
- Liu H, Jia S, Shen D, Liu J, Li J, Zhao H, Han S, Wang Y. 2012. Four AUXIN RESPONSE FACTOR genes downregulated by microRNA167 are associated with growth and development in *Oryza sativa*. *Functional Plant Biology* 39: 736–744.
- Liu H, Wang K, Tang H, Gong Q, Du L, Pei X, Ye X. 2020. CRISPR/Cas9 editing of wheat *TaQ* genes alters spike morphogenesis and grain threshability. *Journal of Genetics and Genomics* 47: 563–575.
- Liu P, Liu J, Dong H, Sun J. 2018. Functional regulation of *Q* by *microRNA172* and transcriptional co-repressor *TOPELESS* in controlling bread wheat spikelet density. *Plant Biotechnology Journal* 16: 495–506.
- Liu R, Hou J, Li H, Xu P, Zhang Z, Zhang X. 2021. Association of *TaD14-4D*, a gene involved in strigolactone signaling, with yield contributing traits in wheat. *International Journal of Molecular Sciences* 22: 3748.
- Liu S, Zhao L, Liao Y, Luo Z, Wang H, Wang P, Zhao H, Xia J, Huang CF. 2020. Dysfunction of the 4-coumarate:coenzyme A ligase 4CL4 impacts aluminum resistance and lignin accumulation in rice. *The Plant Journal* 104: 1233–1250.

- Livak K, Schmittgen T. 2001. Analysis of relative gene expression data using real-time quantitative PCR and the $2^{-\Delta\Delta CT}$ method. *Methods* 25: 402–408.
- Love MI, Huber W, Anders S. 2014. Moderated estimation of fold change and dispersion for RNA-seq data with DESeq2. *Genome Biology* 15: 550.
- Marowa P, Ding A, Kong Y. 2016. Expansins: roles in plant growth and potential applications in crop improvement. *Plant Cell Reports* 35: 949–965.
- Marowa P, Ding A, Xu Z, Kong Y. 2020. Overexpression of *NtEXPA11* modulates plant growth and development and enhances stress tolerance in tobacco. *Plant Physiology and Biochemistry* 151: 477–485.
- Mehrnia M, Balazadeh S, Zanor MI, Mueller-Roeber B. 2013. *EBE*, an AP2/ERF transcription factor highly expressed in proliferating cells, affects shoot architecture in Arabidopsis. *Plant Physiology* 162: 842–857.
- Perestrelo R, Silva P, Porto-Figueira P, Pereira J, Silva C, Medina S, Camara J. 2019. QuEChERS – Fundamentals, relevant improvements, applications and future trends. *Analytica Chimica Acta* 1070: 1–28.
- Pont C, Leroy T, Seidel M, Tondelli A, Duchemin W, Armisen D, Lang D, Bustos-Korts D, Goue N, Balfourier F *et al.* 2019. Tracing the ancestry of modern bread wheats. *Nature Genetics* 51: 905–911.
- Qi Y, Wang S, Shen C, Zhang S, Chen Y, Xu Y, Liu Y, Wu Y, Jiang D. 2012. *OsARF12*, a transcription activator on auxin response gene, regulates root elongation and affects iron accumulation in rice (*Oryza sativa*). *New Phytologist* 193: 109–120.
- Rahmat B, Octavianis G, Budiarto R, Jadid N, Widiastuti A, Matra D, Ezura H, Mubarak S. 2023. *SLIA49* mutation maintains photosynthetic capabilities under heat-stress conditions. *Plants (Basel)* 12: 378.
- Rahmawati S, Chairunnisa C, Erdayani E, Nugroho S, Estiati A. 2019. Overexpression of *OsHox-6* gene enhanced tiller number in rice but induced yield penalty. *Annales Bogorienis* 23: 30–40.
- Sakamoto T, Morinaka Y, Ohnishi T, Sunohara H, Fujioka S, Ueguchi-Tanaka M, Mizutani M, Sakata K, Takatsuto S, Yoshida S *et al.* 2006. Erect leaves caused by brassinosteroid deficiency increase biomass production and grain yield in rice. *Nature Biotechnology* 24: 105–109.
- Shang Q, Wang Y, Tang H, Sui N, Zhang X, Wang F. 2021. Genetic, hormonal, and environmental control of tillering in wheat. *The Crop Journal* 9: 986–991.
- Shao J, Haider I, Xiong L, Zhu X, Hussain R, Overnas E, Meijer A, Zhang G, Wang M, Bouwmeester H *et al.* 2018. Functional analysis of the HD-Zip transcription factor genes *Oshox12* and *Oshox14* in rice. *PLoS ONE* 13: e0199248.
- Shen L, Tian F, Cheng Z, Zhao Q, Feng Q, Zhao Y, Han B, Fang Y, Lin Y, Chen R *et al.* 2022. *OsMADS58* stabilizes gene regulatory circuits during rice stamen development. *Plants (Basel)* 11: 2899.
- Simons K, Fellers J, Trick H, Zhang Z, Tai Y, Gill B, Faris J. 2006. Molecular characterization of the major wheat domestication gene *Q*. *Genetics* 172: 547–555.
- Song G, Sun G, Kong X, Jia M, Wang K, Ye X, Zhou Y, Geng S, Mao L, Li A. 2019. The soft glumes of common wheat are sterile-lemmas as determined by the domestication gene *Q*. *Crop Journal* 7: 113–117.
- Sun J, Cui X, Teng S, Kunnong Z, Wang Y, Chen Z, Sun X, Wu J, Ai P, Quick WP *et al.* 2020. HD-ZIP IV gene *Roc8* regulates the size of bulliform cells and lignin content in rice. *Plant Biotechnology Journal* 18: 2559–2572.
- Sun M, Luo Q, Zheng Q, Tong J, Wang Y, Song J, Zhang Y, Pu Z, Zheng J, Liu L *et al.* 2023. Molecular characterization of stable QTL and putative candidate genes for grain zinc and iron concentrations in two related wheat populations. *Theoretical and Applied Genetics* 136: 217.
- Wang R, Yang X, Guo S, Wang Z, Zhang Z, Fang Z. 2021. MiR319-targeted *OsTCP21* and *OsGAMYB* regulate tillering and grain yield in rice. *Journal of Integrative Plant Biology* 63: 1260–1272.
- Xie L, Liu S, Zhang Y, Tian W, Xu D, Li J, Luo X, Li L, Bian Y, Li F *et al.* 2023. Efficient proteome-wide identification of transcription factors targeting *Glu-1*: a case study for functional validation of TaB3-2A1 in wheat. *Plant Biotechnology Journal* 21: 1952–1965.
- Xing M, Wang W, Fang X, Xue H. 2022. Rice *OsIAA6* interacts with *OsARF1* and regulates leaf inclination. *The Crop Journal* 10: 1580–1588.
- Xu D, Bian Y, Luo X, Jia C, Hao Q, Tian X, Cao Q, Chen W, Ma W, Ni Z *et al.* 2023. Dissecting pleiotropic functions of the wheat green revolution gene *Rht-B1b* in plant morphogenesis and yield formation. *Development (Cambridge, England)* 150: dev201601.
- Yan Y, Ding C, Zhang G, Hu J, Zhu L, Zeng D, Qian Q, Ren D. 2023. Genetic and environmental control of rice tillering. *The Crop Journal* 11: 1287–1302.
- Yang C, Ma Y, Li J. 2016. The rice YABBY4 gene regulates plant growth and development through modulating the gibberellin pathway. *The Journal of Biological Chemistry* 291: 5545–5556.
- Yang X, Hwa C. 2008. Genetic modification of plant architecture and variety improvement in rice. *Heredity* 101: 396–404.
- Yang Y, Li Q, Mu Y, Li H, Wang H, Ninomiya S, Jiang D. 2024. UAV-assisted dynamic monitoring of wheat uniformity toward yield and biomass estimation. *Plant Phenomics* 6: 191.
- Ye Y, Wang S, Wu K, Ren Y, Jiang H, Chen J, Tao L, Fu X, Liu B, Wu Y. 2021. A semi-dominant mutation in *OsCESA9* improves salt tolerance and favors field straw decay traits by altering cell wall properties in rice. *Rice* 14: 19.
- Yoon J, Choi H, An G. 2015. Roles of lignin biosynthesis and regulatory genes in plant development. *Journal of Integrative Plant Biology* 57: 902–912.
- Zhang C, Hegarty J, Padilla M, Tricoli DM, Dubcovsky J, Debernardi JM. 2025. Manipulation of the microRNA172-AP2L2 interaction provides precise control of wheat and triticale plant height. *Plant Biotechnology Journal* 23: 333–335.
- Zhang J, Zhang Y, Xing J, Yu H, Zhang R, Chen Y, Zhang D, Yin P, Tian X, Wang Q *et al.* 2020. Introducing selective agrochemical manipulation of gibberellin metabolism into a cereal crop. *Nature Plants* 6: 67–72.
- Zhang Z, Belcram H, Gornicki P, Charles M, Just J, Huneau C, Magdelenat G, Couloux A, Samain S, Gill B *et al.* 2011. Duplication and partitioning in evolution and function of homoeologous *Q* loci governing domestication characters in polyploid wheat. *Proceedings of the National Academy of Sciences, USA* 108: 18737–18742.

Supporting Information

Additional Supporting Information may be found online in the Supporting Information section at the end of the article.

Fig. S1 Effects of *Q* on plant architecture.

Fig. S2 Field trial comparisons of lodging resistance and spike weight between a representative *Q* knockout line (KO) and negative control wheat cultivar Fielder (NC).

Fig. S3 *Q* binds directly to the promoter of *TaARF12-2A* and regulates its expression.

Fig. S4 Genetic effects of the major haplotypes of *Q* on agronomic traits.

Fig. S5 Genetic effects of the major haplotypes of *TaARF12-2A* on agronomic traits.

Table S1 Primers used in this study.

Table S2 Differentially expressed genes in stem internodes between *Q* knockout lines (KO) and negative control wheat cultivar Fielder (NC).

Table S3 Quantification and comparison of hormones between *Q* knockout lines (KO) and negative control wheat cultivar Fielder (NC).

Table S4 Differentially expressed genes in flag leaves between *Q* knockout lines (KO) and negative control wheat cultivar Fielder (NC).

Table S5 Differentially expressed genes in tiller nodes between *Q* knockout lines (KO) and negative control wheat cultivar Fielder (NC).

Table S6 Quantification and comparison of hormones between *TaARF12-2B* knockout lines (TaARF12-KO) and negative control wheat cultivar Fielder (NC).

Table S7 *Q* haplotypes were defined according to genome resequencing databases in the WheatUnion.

Table S8 Genetic effects of *Q* haplotypes *Hap1* and *Hap2* on agronomic traits in the recombinant inbred lines from the cross Zhongmai 175/Lunxuan 987.

Table S9 *TaARF12-2A* haplotypes were defined according to genome resequencing databases in the WheatUnion.

Table S10 *TaARF12-2B* haplotypes were defined according to genome resequencing databases in the WheatUnion.

Table S11 Genetic effects of the major haplotypes at *TaARF12-2A* on agronomic traits in a diverse panel of 166 wheat cultivars.

Table S12 Genetic effects of major haplotypes of *TaARF12-2B* on agronomic traits in a diverse panel of 166 wheat cultivars.

Table S13 Tetraploid wheats used to trace the origin of *TaARF12-2B-Hap1/2*.

Table S14 Genotyping results of major haplotypes of *TaARF12-2B* in 978 wheat cultivars worldwide.

Table S15 Frequency distributions of favorable haplotypes *TaARF12-2B-Hap1/2* in different continents.

Table S16 Differentially expressed genes in stem internodes between *Q* knockout lines (KO) and negative control wheat cultivar Fielder (NC).

Table S17 Noncoding RNA genes differentially expressed between *Q* knockout lines (KO) and negative control wheat cultivar Fielder (NC) in stem internodes, flag leaves, and tiller buds.

Please note: Wiley is not responsible for the content or functionality of any Supporting Information supplied by the authors. Any queries (other than missing material) should be directed to the *New Phytologist* Central Office.

Disclaimer: The New Phytologist Foundation remains neutral with regard to jurisdictional claims in maps and in any institutional affiliations.